JOURNAL OF KUFA–PHYSICS
journal.uokufa.edu.iq/index.php/jkp/index | ISSN: 2077–5830

Preparation and Photocatalytic Performance of PMMA and ZnO/PMMA Nanocomposite films

Zeina Mossa Dakhel[1] and Khalidah H. Al-Mayalee[2]

[1.2] *Department of Physics, Faculty of Education for Women, University of Kufa, Najaf, Iraq*

[*]*Corresponding Author E-mail:* Zeinam.alrodan@student.uokufa.edu.iq

khalidah.almayali@uokufa.edu.iq

ARTICLE INF.

Article history:
Received: 04 MAR., 2026
Revised: 03 MAY., 2026
Accepted: 06 MAY., 20263
Available Online: 28 JUN. 2026

Keywords:

PMMA/ZnO film;
Dye degradation;
PMMA;
Methylene blue;
ZnO.

ABSTRACT

This study used a simple drop-casting method to create polymethyl methacrylate/zinc oxide (PMMA/ZnO) nanocomposite films. The structural, morphological, and optical properties, and photocatalytic activity of the produced films were studied. X-ray diffraction (XRD) confirmed that pure PMMA is amorphous, while the composite film showed clear peaks for the ZnO hexagonal structure, proving the nanoparticles were added successfully without forming unwanted phases. Scanning Electron Microscopy (SEM) presented that ZnO nanomaterial were spread evenly in the PMMA matrix, changing the surface appearance. Fourier-transform infrared (FTIR) analysis found that PMMA's main functional groups remained after film formation, with a small shift in the carbonyl band in the composite, suggesting a physical interaction between ZnO and the polymer chains. Photoluminescence (PL) spectra showed stronger emission in the nanocomposite films. The films' ability to break down methylene blue (MB) dye was tested under ultraviolet and sunlight. After 60 minutes, the PMMA/ZnO film was broken down to around 69% of the dye under sunlight and 52.5% under UV light. In comparison, pure PMMA broke down 49.5% under sunlight and only 13% under UV. These results show that adding ZnO nanoparticles to PMMA films improves their photocatalytic efficiency, making them promising option for water treatment.

DOI: https://doi.org/ 10.31257/2018/JKP/2026/v18.i1.23713

تولیف وتوصیف وتعزیز النشاط التحفیزي الضوئي لأغشیة PMMA وأغشیة المرکبات النانویة ZnO/PMMA

زینة موسی داخل1 وخالدة ح. المیالي2

قسم الفیزیاء، کلیة التربیة للبنات، جامعة الکوفة، النجف، العراق 1.2

الـــخُـــلاصـــة

الکلمات المفتاحیة:

في هذه الدراسة تم استخدام طريقة الصب بالتنقيط البسيطة لإنتاج أغشية مركبة نانوية من البولي ميثيل ميثاكريلات/أكسيد الزنك .(PMMA/ZnO) تم فحص خصائص الاغشية المحضرة التركيبية والمورفلوجية والبصرية، إضافة الى النشاط التحفيزي الضوئي. أكد تحليل حيود الأشعة السينية (XRD) أن مادة PMMA النقية غير متبلورة، في حين أظهرت الأغشية المركبة قممًا واضحة للهيكل السداسي لأكسيد الزنك، مما يثبت أن الجسيمات النانوية أُضيفت بنجاح دون تكوين مراحل غير مرغوب فيها. أظهر الفحص بالمجهر الإلكتروني الماسح (SEM) أن جسيمات أكسيد الزنك النانوية انتشرت بالتساوي في مصفوفة PMMA، مما أدى إلى تغيير مظهر السطح. وجد تحليل الأشعة تحت الحمراء بتحويل فورييه (FTIR) أن المجموعات الوظيفية الرئيسية لـ PMMA بقيت بعد تكوين الأغشية، مع تحول بسيط في نطاق الكربونيل في المركب، مما يشير إلى تفاعل فيزيائي بين ZnO وسلاسل البوليمر. أظهرت أطياف التألق الضوئي (PL) انبعاثًا أقوى في الأغشية النانوية المركبة. تم اختبار قدرة الأغشية على تحلل صبغة الميثيلين الأزرق (MB) تحت الأشعة فوق البنفسجية وضوء الشمس. بعد 60 دقيقة، حلت طبقة PMMA/ZnO 69% من الصبغة تحت ضوء الشمس و52.5% تحت الأشعة فوق البنفسجية. بالمقارنة، حلت مادة PMMA النقية 49.5% تحت ضوء الشمس و13% فقط تحت الأشعة فوق البنفسجية. تظهر هذه النتائج أن إضافة جسيمات ZnO النانوية إلى طبقات PMMA تحسن كفاءتها للتحفيز الضوئي ، مما يجعلها واعدة في معالجة المياه.

غشاء مركب نانوي من PMMA/ZnO
تحلل الصبغة
PMMA
أزرق الميثيلين
ZnO

1. INTRODUCTION

Industrial wastewater containing synthetic dyes poses a significant environmental challenge due to the high chemical stability and toxicity of these compounds [1]. Methylene blue (MB), widely used in the textile and printing industries, is highly resistant to standard conventional treatments and severely threatens aquatic ecosystems upon release. As a result, there is an urgent and growing need for highly efficient and sustainable wastewater treatment technologies [2]. Photocatalysis has emerged as a highly promising solution for the complete degradation of organic pollutants. It utilizes semiconductor materials that, upon light irradiation, generate electron–hole pairs, leading to the formation of reactive oxygen species (ROS) capable of mineralizing dye molecules into less harmful byproducts [3].

Zinc oxide nanoparticles (ZnO NPs) are widely recognized as an excellent photocatalyst due to their distinct direct optical band gap (~3.37 eV), exceptional chemical stability, non-toxicity, and strong ultraviolet (UV) absorption capabilities [4]. However, the practical large-scale application of bare ZnO nanoparticles is often hindered by their tendency to agglomerate, difficulty in post-treatment recovery, and limited mechanical stability when used alone. To overcome these critical limitations, embedding ZnO NPs into a robust polymer matrix, such as polymethyl methacrylate (PMMA), provides an effective strategy. PMMA is a highly transparent and chemically stable polymer with excellent film-forming properties, ensuring improved nanoparticle dispersion, mechanical durability, and ease of handling, making it an ideal host matrix for hybrid nanocomposites designed for advanced environmental applications [5].

Therefore, the primary objective of this study is to develop a highly efficient, scalable, and practically deployable photocatalytic platform by fabricating PMMA/ZnO nanocomposite films using a facile and cost-effective drop-casting technique. To highlight the practical contribution

and significance of this work, the structural, optical, and morphological properties of the fabricated films were systematically investigated and correlated with their photocatalytic performance. Specifically, the novelty of this study lies in utilizing these stable, easily recoverable, and free-standing solid films to achieve significantly enhanced degradation of MB dye under both UV and natural sunlight irradiation, thereby offering a sustainable, economical, and large-scale applicable solution for industrial wastewater remediation.

2. Experimental Work

2. 1 Drop Casting methods

A simple method was used to fabricate the photocatalytic films. Before the deposition process, glass substrates were cleaned with distilled water and ethanol, followed by ultrasonication for 15 minutes to clean them of impurities. The substrates were then dried in a thermal oven at 90°C for 30 minutes. Before the drop casting stage begins, to determination the deposited film's mass, the substrates are weighed using a sensitive scale before and after casting process. Aso, the solution density can be determined by weighing the container before and after filling with a known volume. The dimensions of the used substrates were 2 × 2.5 mm and ranging in thickness from 1.0 mm to 1.2 mm. Based on these gravimetric measurements and the known surface area of the substrate (A), the average thickness (t) of the fabricated nanocomposite films was calculated using the following standard gravimetric relationship [6, 7]:

$$(t = \frac{m}{A \cdot \rho})$$

2.1.1 Preparation of PMMA Films:

A white powder of Polymethyl methacrylate (PMMA) polymer (from otto bock Health Care, German) and 350,000 g/mol molecular weight were used to prepare PMMA films and PMMA/ZnO NPs composite films using drop casting method. The polymer density was 0.85 g/cm3. Initially, PMMA/acetone solution was prepared by distilled wight (1 g) of PMMA polymer powder in 50 ml volume of acetone and stirred for 2h at 50○C on magnetic stirrer until the polymer was completely dissolved, resulting in a clear and homogeneous solution of polymer with 2.48 weight ratio. After that the drop casting process used to synthesis PMMA film by using 10 ml of each polymer concentration. The solution was distilled in volume of 0.5 ml for each slide in three stages to obtain layers of the membrane between each layer. The sample was placed in a thermal controlled oven at 90 ○C for 5 minutes.

2.1.2 Preparation of PMMA/ZnO NPs Composite Films:

The drop-casting processing method was used to deposit PMMA/ZnO nanocomposite films onto glass substrate. PMMA/ZnO nanocomposite solution was prepared by incorporating ZnO nanoparticles (0.1 g) into a host polymer/acetone solution with a 2.48 weight ratio. The

nanoparticles were added gradually under continuous magnetic stirring to prevent agglomeration and ensure a uniform distribution of the ZnO NPs (0.1g) within 1g PMMA matrix. Following a specific duration of ultrasonication, a stable and homogeneous nanocomposite solution was obtained, ready for drop casting deposition process. A multi-stage drop-casting technique was employed by dispensed the prepared solutions in three sequential steps (0.5 ml per layer) to achieve a uniform and controlled film layer thickness.

Figure 1: The synthesized film samples after drying

Among each deposition, the substrates were annealed in a thermal oven at 90°C for three minutes to ensure complete solvent evaporation and minimize impurities, resulting in high-quality, dense nanocomposite films. The final weight percentages of ZnO nanoparticles (0.1g) in the PMMA matrix (1g) after solvent evaporation was 9.10 wt%. After drop casting and drying processes, the polymer and composite membranes were weighed, washed with distilled water, and carefully scraped from the substrate, as shown in Figure (1)

2.2 Preparation of Contaminated Dye Concentration:

Methylene blue dye was prepared in double-distilled water. The stock solutions were prepared with a constant concentration of 1.8×10-3 molar for all samples.as shown in the image below:

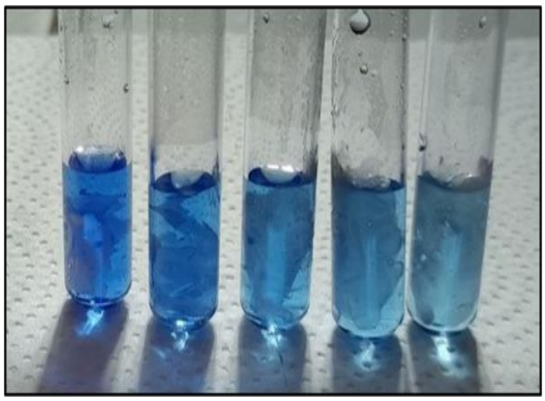

Figure 2: Prepared samples for photocatalysis, showing a clear color change indicating dye degradation after the photocatalysis process.

2.3 Characterization Techniques

The crystal structure of the created samples was determined by XRD. The optical properties were investigated through an optical (UV-Vis) spectroscopy within the wavelength range of 200 to1100 nm. Scanning Electron Microscopy (SEM) was employed to describe the nature of the surface and determine the shape and distribution of nanoparticles within the polymer matrix. Finally, the photocatalytic performance of the fabricated films was evaluated by monitoring the photodegradation efficiency of Methylene Blue dye under both UV and sunlight irradiation.

2.4 Results and Discussion

2.4.1 Optical Spectroscopic analysis

The absorbance curve of the PMMA and PMMA/ZnO NPs composite films as a function of wavelength in the range of 200 to 800 nm are presented in figure 3. As shown in the figure, the PMMA film with 238 µm thick exhibits weak absorption in the visible region and near UV region with a sharp absorption edge starting around 290 nm. This behavior is expected for PMMA, a transparent polymer with a wide energy gap, which does not absorb visible light. The absorbance spectrum of the PMMA/ZnO nanocomposite film with 236 µm thick showed enhanced and sustained absorption in the near-UV region and extending further [8]. This corresponds to the band edge absorption of ZnO NPs with an energy gap (about 3.2 eV). This indicated that the ZnO NPs (0.1g) are well dispersed within the polymer matrix, while maintaining good transparency in visible light.

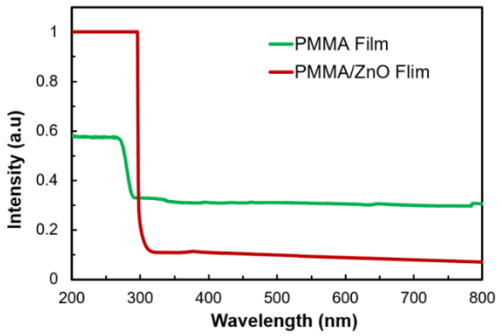

Figure 3: UV-visible absorbance of PMMA (1g) film and PMMA/ZnO (0.1g) NPs composite film

The direct energy gap (Eg) values of the PMMA (1g) and PMMA (1g)/ ZnO (0.1g) nanocomposite film with a thickness of about (236 µm) and 280 µm respectively, were calculated by using the were the Tauc plot method, based on the equation $[(\alpha h\nu)]^2=B(h\nu-E_g)$, where (B) is constant, (hv) is the energy of the incident photon, and (α) is the absorption coefficient and can be can be written as ($\alpha=(2.303*A)/d$) , (d) is the film thickness [8] and presented in Figure 4. The results shown in Figure 4 revealed that the band gap of the PMMA polymer film was 4.21 eV and the optical band gap of PMMA/ ZnO nanocomposite film recorded (4.18 eV) value and. The value of PMMA/ ZnO NPs film is greater than the gap of pure ZnO (3.2 eV) and less than the gap of pure PMMA. This increase is due to the quantum size effect of ZnO nanoparticles, the dielectric matrix (PMMA) effect, and absence of charge transfer. Similar energy gaps were observed in PMMA/ ZnO NPs films in the literature [9].

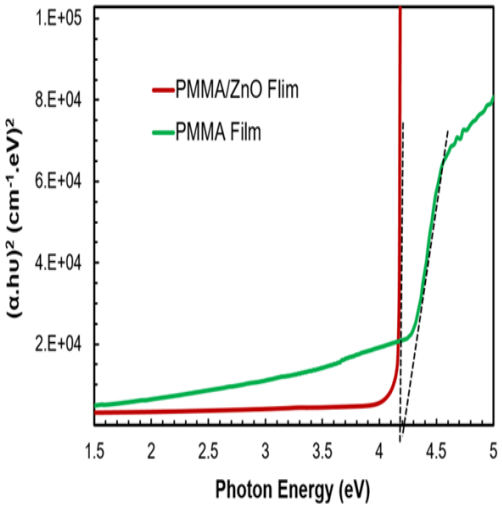

Figure 4: Energy gap of PMMA (1g)/ZnO (0.1 g) nanocomposite film

2.4.2 PL Spectroscopy Analysis

Photoluminescence (PL) spectra of pure PMMA and the PMMA/ZnO NPs

composite films showed in Figure 5. PMMA film exhibited a relatively weak and broad emission peak at 350–380 nm, representing $\pi \rightarrow \pi^*$ electronic transitions in the carbonyl group (C=O), which are well-known emissions in amorphous PMMA chains. The spectrum also decreases rapidly beyond 400 nm due to the film's low photoactivity compared to solutions, acting primarily as a transparent host for the inorganic fillers [10].

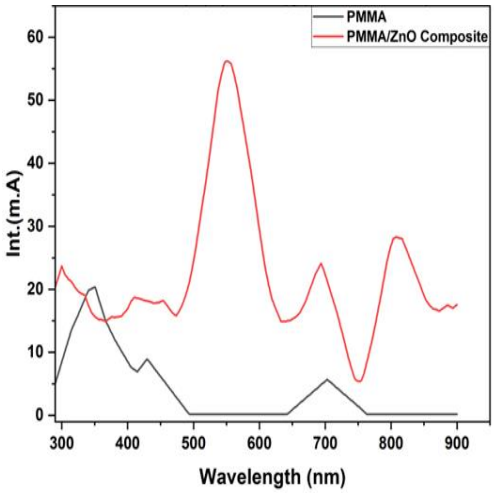

Figure 5: PL emission spectra of PMMA and PMMA/ZnO composite samples.

Figure (5) revealed the significant improvement in emission peaks of the PMMA/ZnO NPs composite PL curve compared to the pure PMMA. The first peak appears at ~340 nm in a ultraviolet region, and this due to the near-band edge exciton recombination of the ZnO NPs. The second distinct and enhanced peak at ~560 nm corresponding to deep-level oxygen vacancy defects. Also, there is a characteristic emission near-infrared region at ~815 nm. [11] PMMA/ZnO film exhibits strong PL peaks in the visible and near-infrared regions due to crystal defects in ZnO and energy transfer from PMMA, demonstrating the formation of an optically active compound suitable for low-power optics applications. PMMA film alone shows weak and limited emission only in the violet region.

2.4.3 FTIR Spectra

The recorded FTIR spectrum of the PMMA polymer and PMMA/ZnO composite films are included in Figure (6). The chemical interactions and functional groups within the of PMMA polymer appears in both PMMA and the PMMA/ZnO samples, including the broad hydroxyl (O-H) stretching group at ~3439 cm^{-1}, aliphatic C-H groups appear at ~2990 cm^{-1}, and the sharp, high intensity peak at ~1735 cm^{-1} which is attributed to the tensile carbonyl group (C=O) vibration. [12] However, the interaction between ZnO and PMMA matrix produces noticeable shifts and intensity changes in the FTIR spectrum, particularly in the lower wavenumber region. This behavior corresponds to the characteristic Zn–O metal-oxide stretching vibration. Furthermore, the slight shift in the carbonyl and ether (C–O–C) peaks at 1147 cm^{-1} suggests a strong interfacial interaction and hydrogen bonding interactions between ZnO NPs surface and PMMA matrix. These spectral features confirm the effective nanoparticles integration with the polymer host matrix and formation a stable nanocomposite structure without the emergence of unexpected chemical impurities [13].

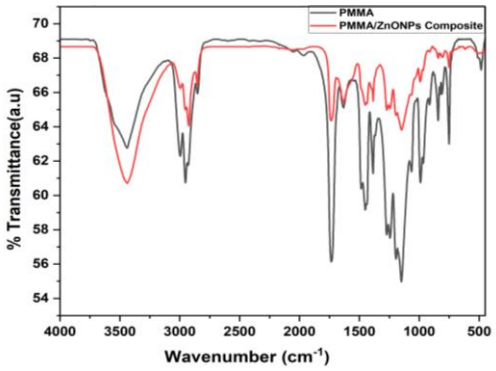

Figure 6: FTIR Spectra of PMMA, and PMMA/ZnO composite

2.4.4 XRD Analysis

The XRD patterns of the prepared PMMA and PMMA/ZnO films are demonstrated in Figure (7). The pure PMMA film exhibits amorphous nature and the disordered arrangement of its polymer chains. This behavior is consistent with what is documented for PMMA polymer in the scientific literature [14]. In contrast, the PMMA/ZnO film demonstrated sharp and distinct diffraction peaks at angles of approximately The PMMA/ZnO film exhibited pronounced and well-defined diffraction peaks at angles of approximately 31.6°, 34.2°, 36.2°, 47.3°, 56.35°, 62.65°, 66.4°, 67.75°, and 68.9° corresponding to the (100), (002), (101), (102), (110), (103), (200), (112), and (201) crystal planes, respectively. These values indicate the polycrystalline nature of ZnO NPs and represented to be the hexagonal wurtzite structure (JCPDS card no. 36-1451). The results of XRD analysis indicate the successful incorporation in the PMMA matrix without any secondary phases appearing [15].

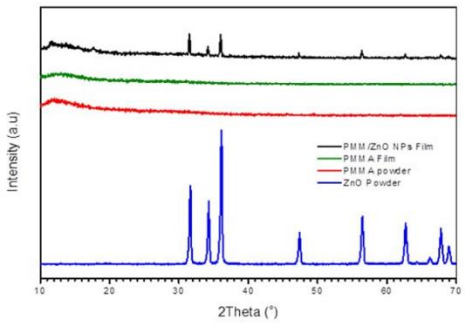

Figure 7: X-ray diffraction of the PMMA and ZnO/PMMA composite film.

2.4.5 Morphology Analysis

Figure 8 (a) displays the scanning electron microscopy (SEM) image of the pristine PMMA film, revealing an interconnected network of polymer fibers with a highly porous architecture. This morphology is characteristic of amorphous PMMA polymer membranes [16]. Conversely, Figure 8 (b) demonstrates that the PMMA/ZnO nanocomposite film exhibits a drastically altered topography, featuring a more continuous, densified, and cohesive surface with distinct micro-pores distributed across the film. The altered surface morphology is primarily attributed to the uniform dispersion and embedding of ZnO nanoparticles within the polymer matrix. The incorporation of ZnO NPs effectively filled the interstitial spaces of the original fibrous network, leading to a highly integrated and densified composite structure [17, 18]. While the dense polymer coating and the micro-scale resolution restrict the direct measurement of individual nano-sized ZnO particles from these specific micrographs, the overall structural transformation successfully confirms

the excellent integration of the filler within the matrix without macroscopic phase separation.

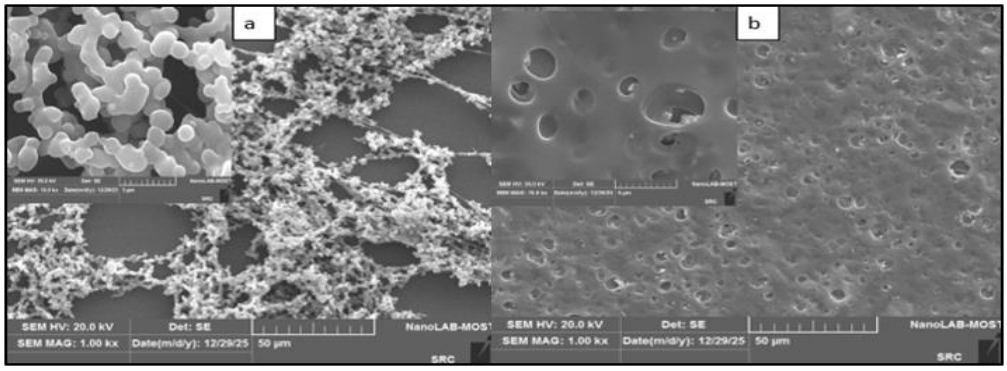

Figure 8: SEM photograph the (a) PMMA film (b) PMMA/ZnO composite film.

2.4.6 Photocatalytic Application

The photocatalytic efficiency of PMMA and PMMA/ZnO films with thicknesses of about 238 µm and 236 µm, respectively, was evaluated by monitoring the absorbance spectra of Methylene Blue dye under UV light irradiation as shown in figure (9) for different irradiation times (0, 15, 30, 45, 60 min). The experimental results in figure 9 revealed that the pure PMMA films exhibit reasonable photocatalytic activity under UV light [19]. The photodegradation was calculated using the relationship ((A_0.-A)/A_0 ×100 % ,A_0 is the initial MB centration), and its value was of the pure polymer film was about 23.5 % after one hour of UV irradiation, with reaction rate constant (k) of 0.0045 min-1 (Table 1). These enhanced results are primarily attributed to the direct photolysis of the dye under UV light and physical adsorption onto the porous polymer surface [20].

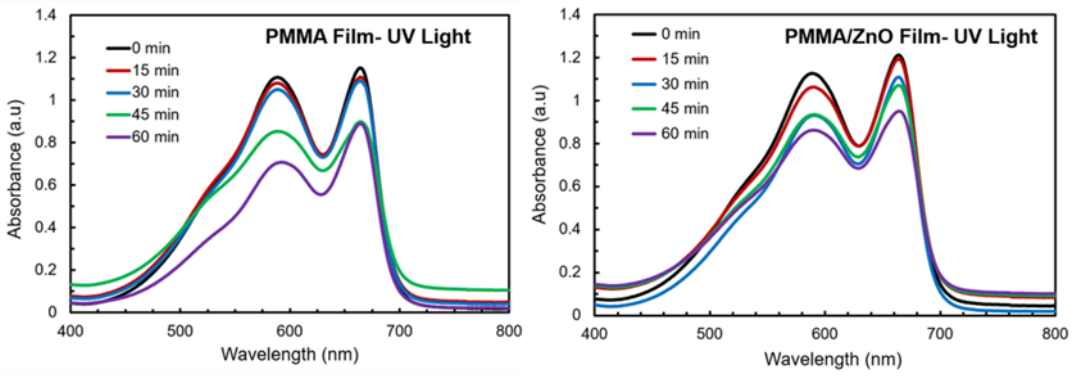

Figure 9: Absorption spectra of methylene blue and its photocatalytic degradation profiles using PMMA film, and PMMA/ZnO nanocomposite film under UV light for different irradiation times.

Figure (9) also illustrates the PMMA/ZnO nanocomposite film photocatalytic response over time with low degradation efficiency reached to

21.5% and the rate constant (k) about 0.0043 min^{-1}. The marked decrease in the photo-degradation efficiency value for the PMMA (1g)/ZnO NPs (0.1g) film compared to the pure PMMA film might be attributed to the wight variation of component, ZnO particles may cluster in small area (defects) within the polymer and act as light scattering centers, resulting in a relative decline in overall photocatalytic performance [21].

The photocatalytic performance of the pure PMMA and PMMA/ZnO nanocomposite films was further investigated under natural sunlight irradiation, as shown in figure (10). The experimental results illustrated a remarkable difference in performance compared to the UV-light results. The pure PMMA film showed an acceptable absorbance of the MB over 60 minutes. This is due to the wide spectrum of sunlight, which includes UV radiation that leads to self-photolysis of the dye, in addition to the thermal effect of the solar radiation, which may enhance the adsorption of the dye on the porous polymer surface [20]. The calculated degradation efficiency value of the PMMA film under natural sunlight was 47.1% and a rate constant of 0.0106 min^{-1} as shown in Table 1. This performance significantly outperforms that of the polymer film under artificial UV light, due, as mentioned previously, to the broad spectrum of sunlight and the solar thermal effect, which promotes faster dye adsorption [22]. On the other hand, The PMMA/ZnO film exhibited a significantly enhanced performance, with the degradation efficiency value increasing to 56% and the rate constant value was 0.0137 min^{-1} under sunlight.

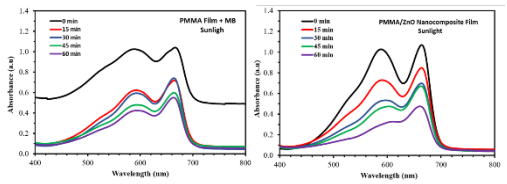

Figure 10: Absorption spectra of methylene blue and its photocatalytic degradation profiles using PMMA Film and PMMA/ZnO nanocomposite film under sunlight for different irradiation times.

Table 1: Absorption values, the rate of decomposition, and the degradation reaction rate of methylene blue dye using PMMA Film, and PMMA/ZnO NPs composite film under sunlight and UV light.

Film Sample	A_0 (at 0 min)	A (at 60 min)	Decay ratio %	k *10^{-3} $(min)^{-1}$
Under sunlight				
PMMA	1.04	0.55	47.1	**10.62**
PMMA/ZnO Nanocomposite	1.07	0.47	56.0	**13.7**
Under UV light				
PMMA	1.15	0.88	23.5	**4.46**

PMMA/ZnO Nanocomposite	1.21	0.95	21.5	**4.03**

Figure 11 shows that the degradation efficiency under UV and natural sunlight light of the film samples increases with increasing exposure time to light, and the PMMA/ZnO nanocomposite exhibited faster under sunlight than UV light. The results show that the best catalytic performance is achieved when the ZnO NPs are combined with PMMA polymer under sunlight, due to its homogeneous distribution of ZnO nanoparticles and small size, which improves electron transfer efficiency. However, the PMMA/ZnO nanocomposite film has a larger surface area that allows for greater absorption of visible light, making it particularly effective with methyl blue dye that interacts strongly with light [22]. The results highlight the potential of using PMMA/ZnO NPs films as effective catalysts in the treatment of wastewater containing organic dyes, particularly when utilizing natural sunlight.

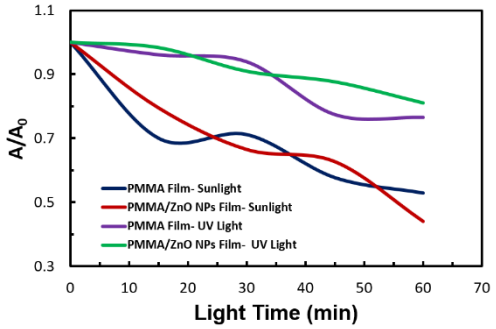

Figure 11: The degradation efficiency rate of PMMA and PMMA/ZnO nanocomposite films as a function of exposure UV and sunlight light time.

Conclusions

Thin films of pure polymer (PMMA) films and a composite film PMMA/ZnO NPs films were successfully fabricated using the drop-casting method. The study showed that the incorporation of zinc oxide nanoparticles into the polymer matrix significantly alters its structural and functional properties. X-ray diffraction (XRD) analysis confirmed the amorphous structure of the PMMA polymer alongside the pure hexagonal crystalline phase of the ZnO nanoparticles, indicating successful dispersion of the nanoparticles without the formation of secondary phases. Scanning electron microscopy (SEM) images also revealed a porous surface structure ideal for dye adsorption and light trapping, while FTIR results indicating the effective incorporation of nanoparticles. The photoluminescence (PL) spectra identifying fundamental oxygen vacancies that facilitate charge separation. The pure polymer film exhibited acceptable efficiency under both light sources driven by direct photodegradation of the dye and physical adsorption. Whereas, the PMMA/ZnO composite films showed a slight decline in performance under UV light, which is attributed to variations in the weights of the components and the agglomeration of ZnO particles in limited areas, causing them to act as light-scattering centers rather than absorbing light. In contrast, the composite film achieved significantly superior and enhanced performance under natural sunlight, outperforming

the pure film under sunlight (which, in turn, benefited from the broad spectrum of sunlight and the thermal effect in accelerating adsorption). This superior performance of the composite film under sunlight is attributed to the homogeneous distribution and small size of the nanoparticles, which improved electron transport, as well as the large surface area that allowed for higher absorption of visible light. These results confirm that the best synergy between the polymer and the nanoparticles is achieved under natural sunlight, making the PMMA/ZnO nanocomposite films a promising and highly effective material for environmental applications, including the treatment of water contaminated with organic pollutants.

Acknowledgments

The authors would like to express their gratitude to the physics department staff, Faculty of Education for women, university of Kufa for their moral support in completing this work.

References

[1] Robinson, T., McMullan, G., Marchant, R., & Nigam, P. (2001). Remediation of dyes in textile effluent: a critical review on current treatment technologies with a proposed alternative. Bioresource technology, 77(3), 247-255.

[2]Forgacs, E., Cserháti, T., & Oros, G. (2004). Removal of synthetic dyes from wastewaters: a review. Environment international, 30(7), 953-971 .

[3]Özgür, Ü., Alivov, Y. I., Liu, C., Teke, A., Reshchikov, M. A., Doğan, S., ... & Morkoç, A. H. (2005). A comprehensive review of ZnO materials and devices. Journal of applied physics, 98 .(4)

[4]Klingshirn, C. (2007). ZnO: From basics towards applications. physica status solidi (b), 244(9), 3027-3073 .

[5]Dhand, C., Dwivedi, N., Loh, X. J., Ying, A. N. J., Verma, N. K., Beuerman, R. W., ... & Ramakrishna, S. (2015). Methods and strategies for the synthesis of diverse nanoparticles and their applications: a comprehensive overview. Rsc Advances, 5(127), 105003-105037 .

[6]Ohring, M. (2001). Materials Science of Thin Films: Deposition and Structure (2nd ed.). Academic Press.

[7]Beaucage, G., Composto, R. J., & Stein, R. S. (1993). Ellipsometric and gravimetric determination of thin-film thickness in polymer blends. Journal of Polymer Science Part B: Polymer Physics, 31(3), 319-326.

[8]Wang, L. (2014). Preparation and luminescent properties of ZnO quantum dots nanocomposites (Doctoral dissertation).

[9]Okur, S., Shimada, R., Zhang, F., Hafiz, S. D. A., Lee, J., Avrutin, V., ... & Özgür, Ü. (2013). GaN-based vertical cavities with all dielectric reflectors by epitaxial lateral overgrowth. Japanese Journal of Applied Physics, 52(8S), 08JH03.

[10] Özgür, Ü., Hofstetter, D., & Morkoc, H. (2010). ZnO devices and

applications: a review of current status and future prospects. Proceedings of the IEEE, 98(7), 1255-1268.

[11]Socrates, G. (2004). Infrared and Raman characteristic group frequencies: tables and charts. John Wiley & Sons .

[12]Klingshirn, C. (2007). ZnO: From basics towards applications. physica status solidi (b), 244(9), 3027-3073 .

[13]El-Zaher, Nabawia A., Mohamed S. Melegy, and Osiris W. Guirguis. "Thermal and structural analyses of PMMA/TiO2 nanoparticles composites." Natural Science 6.11 (2014): 859 .

[14]Özgür, Ü., Alivov, Y. I., Liu, C., Teke, A., Reshchikov, M. A., Doğan, S., ... & Morkoç, A. H. (2005). A comprehensive review of ZnO materials and devices. Journal of applied physics, 98 .(4)

[15]Baker, R. W. (2023). Membrane technology and applications. John Wiley & Sons .

[16]Kołodziejczak-Radzimska, A., & Jesionowski, T. (2014). Zinc oxide—from synthesis to application: a review. Materials, 7(4), 2833-2881 .

[17]Kołodziejczak-Radzimska, A., & Jesionowski, T. (2014). Zinc oxide—from synthesis to application: a review. Materials, 7(4), 2833-2881 .

[18]Sirelkhatim, A., Mahmud, S., Seeni, A., Kaus, N. H. M., Ann, L. C., Bakhori, S. K. M., ... & Mohamad, D. (2015). Review on zinc oxide nanoparticles: antibacterial activity and toxicity mechanism. Nano-micro letters, 7(3), 219-242 .

[19] Wang, L. (2014). Preparation and luminescent properties of ZnO quantum dots nanocomposites (Doctoral dissertation).

[20] Kulis-Kapuscinska, A., Kwoka, M., Borysiewicz, M. A., Wojciechowski, T., Licciardello, N., Sgarzi, M., & Cuniberti, G. (2023). Photocatalytic degradation of methylene blue at nanostructured ZnO thin films. Nanotechnology, 34(15), 155702.

[21] Wang, L. (2014). Preparation and luminescent properties of ZnO quantum dots nanocomposites (Doctoral dissertation).

[22] Kulis-Kapuscinska, A., Kwoka, M., Borysiewicz, M. A., Wojciechowski, T., Licciardello, N., Sgarzi, M., & Cuniberti, G. (2023). Photocatalytic degradation of methylene blue at nanostructured ZnO thin films. Nanotechnology, 34(15), 155702.